Available online at www.sciencedirect.com
ScienceDirect
Scripta Materialia 65 (2011) 367–370
Scripta MATERIALIA
www.elsevier.com/locate/scriptamat

Origination of electron magnetic chiral dichroism in cobalt-doped ZnO dilute magnetic semiconductors

Z.H. Zhang,[a,c,*] H.L. Tao,[a] Ming He[b] and Quan Li[c]

[a]*Liaoning Key Materials Laboratory for Railway, School of Materials Science and Engineering, Dalian Jiaotong University, Dalian 116028, China*
[b]*Department of Physics, Dalian Jiaotong University, Dalian 116028, China*
[c]*Department of Physics, The Chinese University of Hong Kong, Shatin, New Territory, Hong Kong SAR, China*

Received 7 April 2011; revised 5 May 2011; accepted 6 May 2011
Available online 14 May 2011

Electron magnetic chiral dichroism (EMCD) relates the microstructure of a single nanostructure with the magnetic property, indicating that the ferromagnetism observed in cobalt-doped ZnO dilute magnetic semiconductor is intrinsic. First-principles calculations were carried out and the electronic states contributing to the spin imbalance are identified. An exact model is developed, allowing one to visualize the origination of dichroism to be the difference of transition intensity from spin-polarized 2*p* states to Co-3*d* states in cobalt-doped ZnO nanostructures.

Keywords: Electron energy loss spectroscopy (EELS); First-principles electron theory; Semiconductor compounds; Nanostructure

Dilute magnetic semiconductors (DMS), in which non-magnetic semiconductors are doped with a few percent of magnetic atoms, have attracted intensive research interest due to their potential applications in spintronic devices [1]. Transition metal-doped ZnO, one of the most studied DMS systems, has become a focus of attention due to the observation of its room-temperature ferromagnetism [2–4]. Although a large number of studies on transition metal-doped ZnO are available in the literature, there is no consensus on whether the observed ferromagnetism is intrinsic [5,6]. Especially for DMS nanostructures, the measurement of magnetic properties is performed on a large number of nanostructures. How to relate the microstructure of a single nanostructure with the magnetic property of the same nanostructure is a major challenge.

Dichroism, an important magnetic–optic property of DMS, refers to changes in the absorption of left- and right-polarized light when passing through the DMS material. The measurement of dichroic signals reflects the anisotropy of the spin in the material and thus can be regarded as an efficient method to identify the intrinsic ferromagnetism in ZnO-based DMS [6]. Electron magnetic chiral dichroism (EMCD), performed in transmission electron microscopy (TEM), is the difference in the transition metal-$L_{2,3}$ edges collected under two opposite chirality conditions [7] (the electron beams under two opposite chirality conditions are comparable to the left- and right-polarized light). When EMCD experiments are performed, the microstructure of the same nanostructure can be detected simultaneously by TEM-related techniques. Thus, EMCD results provide direct evidence of intrinsic ferromagnetism in individual DMS nanostructures [8].

Despite all these experimental studies, an exact model is still required, and urgently needed, to illustrate the experimentally observed dichroism in ZnO-based DMS. The dichroism reflects the magnetic property of ZnO-based DMS and the magnetic property is determined by the spin imbalance of the materials. Thus, if the electronic states contributing to the spin imbalance can be identified, the origination of the dichroism in DMS could be understood. Consequently, a clear and direct connection between dichroism and the electronic structure of transition metal-doped ZnO would be established.

In this work, we tackled the above problem by using a cobalt-doped ZnO nanostructure as the model system.

* Corresponding author at: Liaoning Key Materials Laboratory for Railway, School of Materials Science and Engineering, Dalian Jiaotong University, Dalian 116028, China. Tel.: +86 411 84105700; fax: +86 411 84109417; e-mail: zhzhang@djtu.edu.cn

1359-6462/$ - see front matter © 2011 Acta Materialia Inc. Published by Elsevier Ltd. All rights reserved.
doi:10.1016/j.scriptamat.2011.05.013

EMCD experiments were performed to prove the intrinsic ferromagnetism of the studied DMS material. The electronic structures of cobalt-doped ZnO were obtained from first-principles calculations, and the electronic states contributing to the spin imbalance were identified from the calculated density of states. To correlate the dichroism observed in cobalt-doped ZnO with its electronic structure, an exact model is proposed and correspondingly the origination of dichroism in cobalt-doped ZnO DMS can be deduced.

The studied Co-doped ZnO nanoparticles were synthesized by a simple solvothermal technique [9]. Typical morphologies of the Co-doped ZnO nanoparticles are shown in Figure 1a. No clustering of the Co is observed. Co concentrations were estimated by energy-dispersive X-ray spectroscopy (EDS) as ~6%. The samples exhibit well-defined hysteresis loops, which demonstrated a robust high-temperature (300 K) ferromagnetic behavior, as shown in Figure 1b. The observed ferromagnetism of the studied cobalt-doped ZnO system has been proved to be intrinsic by X-ray photoelectron spectroscopy [9], atom location by channeling enhanced microanalysis [8], spatially resolved electron energy loss spectroscopy [9,10] and EMCD [8]. The EMCD measurements were performed at "+" and "−" positions in the diffracted pattern to show opposite chirality conditions [7] (the inset of Fig. 1d) with either the objective lens (with a magnetic field of ~2 T exerted on the specimen) or the Lorentz lens (objective lens off, with a small magnetic field of ~17 Oe) [8]. The data shown in Figure 1c and d are EMCD spectra obtained with an objective lens and a Lorentz lens, respectively. For both the objective lens on and off cases, the intensity of the Co-L_3 edge taken at the "+" position is higher than that taken at the "−" position, which is the opposite of the L_2 edge. So dichroism effects (at the bottom of Fig. 1c and d) are observed both under a magnetic field and after removing the magnetic field, which means that the ferromagnetism in the cobalt-doped ZnO investigated is intrinsic [8]. One should note that there is a difference between the macroscopic measurement (Fig. 1b) and the EMCD results (Fig. 1c and d). For the macroscopic measurement, the magnetization is almost saturated at 2 T, but is negligible at 17 Oe. However, the EMCD signals between the "+" and "−" spectra are not very different between Figure 1c and d. On the macroscopic scale, the whole sample can be treated as an ensemble composed of different magnetic domains. For the EMCD measurement, only a local area of a single nanoparticle was probed, so the dichroism signal represents the magnetization of the local region. If the net moment in the probed area is aligned to a direction either parallel or antiparallel to the incident electron beam, a maximum dichroism can be achieved. Therefore, one should expect to see a difference between the macroscopic (Fig. 1b) and microscopic measurements (Fig. 1c and d).

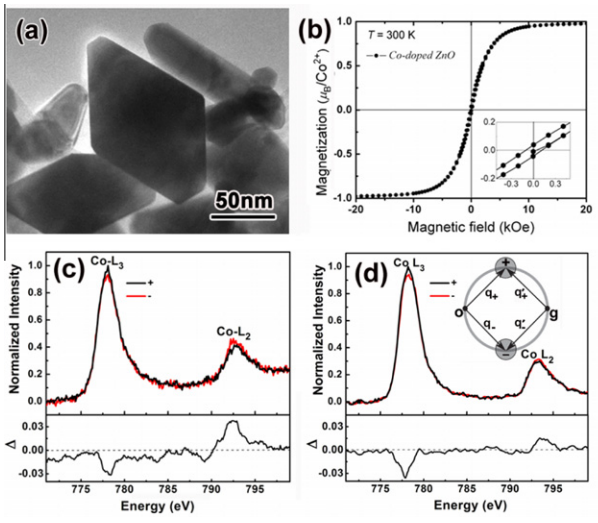

Figure 1. (a) Low-magnification TEM images of the Co-doped ZnO sample; (b) magnetic hysteresis loops measured at 300 K. The inset shows the enlargement of the hysteresis loops near the origin; (c) EMCD results of the Co-doped ZnO samples obtained under the objective lens; (d) EMCD results of the Co-doped ZnO samples obtained under the Lorentz lens. The Co-$L_{2,3}$ edges were taken from two chiral positions "+" and "−", as indicated by the inset.

Motivated by these experimental results, the calculations with a Co doping concentration of 6.25% (close to the experimental concentration) were performed. One zinc atom is replaced by cobalt in a $2 \times 2 \times 2$ supercell of the hexagonal ZnO ($Zn_{15}Co_1O_{16}$) and the structure was optimized until the net force on each atom was smaller than 0.01 eV Å^{-1}. The electronic structure calculations were performed using the highly accurate all-electron full-potential linearized augmented plane-wave method implemented in the WIEN2K Package [11] within the generalized gradient approximation [12]. The size of the basis sets was controlled by the parameter $R_{mt}K_{max}$, where R_{mt} is the smallest muffin tin radius in the unit cell and K_{max} is the magnitude of the largest **K** vector in reciprocal space. In our calculations, $R_{mt}K_{max}$ was taken to be seven. The number of k-points in the whole Brillouin zone was increased until the total energy had converged.

Figure 2a and b shows the calculated total and projected density of states (DOS) without and with involving spin polarization, where the Fermi level is set at zero. The local d orbitals of the Co atom are introduced into the gap of the host semiconductor ZnO. The majority spin (↑) 3d states of Co located between ~−1 and ~−2 eV are t_2 states, and the Fermi level cuts the sharp minority spin (↓) e states. The minority spins t_2 states of Co (higher in energy than the e states) are seen to be hybridized slightly, with the conduction band and the DOS near the Fermi level indicating the presence of a half-metallic character. The host's valence band maximum is composed of O-p bands and Zn-d bands, which is lower than the localized Co-3d orbitals. For both Zn-d and O-p, the density of states between −5 and −1 eV changed from symmetry (corresponding to the ZnO case [13]) to asymmetry (to Co-doped ZnO). That is, the spin splitting are observed in both O-p and Zn-d bands due to the exchange interaction with the doped Co, which can be seen clearly from the projected density of states of the O-p and Zn-d states. For the O-p band, the density of states between −2 and 2 eV is very similar to the cobalt-d states, indicating the strong exchange interaction between the O-2p and Co-3d states. The most prominent unoccupied energy bands in the conduction

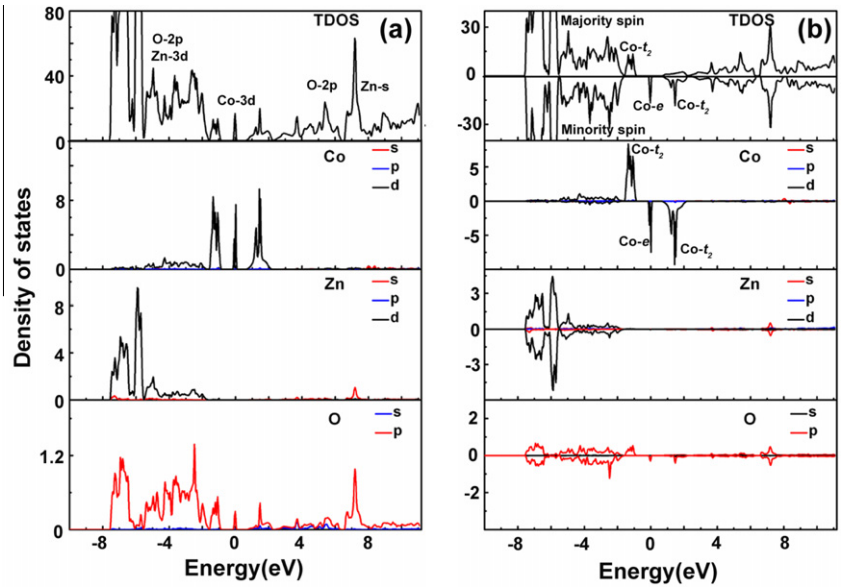

Figure 2. The calculated total density of states (TDOS) and projected density of states (PDOS) of Co-doped ZnO (the Co concentration of 6.25%). (a and b) Results without and with involving spin polarization, respectively.

band are composed of Zn-*s* and O-*p* states. The calculated results are consistent with that calculated by Vienna Ab Initio Simulation Package [10,14].

Based on the calculations, an exact model to illustrate the origin of the dichroic signals in the Co-$L_{2,3}$ edges of Co-doped ZnO is given in Figure 3. For conventional Co-$L_{2,3}$ edges recorded under non-chirality conditions (shown as below in Fig. 3a), they originate from electronic transitions from the 2*p* states (the red filled area in Fig. 3a) to empty Co-3*d* states (the blue filled area in Fig. 3a) above the Fermi level. There is no need to rotate spin polarization when the conventional electron energy loss spectroscopy data are correlated with the electronic structure of the DMS. The transition intensity from the O-2*p* state to the Co-3*d* state, measured as the white line intensity $I_{L_3} + I_{L_2}$, is proportional to the number of *d* holes [15]. When the EMCD experiments were performed, seen at the bottom of Figure 3b, the electron energy loss spectra were recorded under the opposite chirality conditions (corresponding to the "+" and "−" positions in the diffraction pattern). The interaction between the incident electrons and the *p*-electrons (in the material) leads to the excitation of spin-polarized electrons, so spin-polarized DOS have to be involved. At the "−" position, fewer spin-up electrons and more spin-down electrons are excited, while at the "+" position, more spin-up and fewer spin-down electrons are excited. As seen in Figure 3b, there are more empty spin-down states (mainly from the Co-*e* and Co-t_2 states) than empty spin-up states. Correspondingly, when the experiments were performed at spin down "−" position, more spin-down electrons are excited from the 2*p* state to the more empty Co-3*d* spin-down states. The absorption is larger and consequently the intensity of L_2 is higher, which is the opposite of the L_3 edge. Just the difference in transition intensity for the spin-up and spin-down electrons leads to the observation of dichroic signals at the $L_{2,3}$ edges of Co.

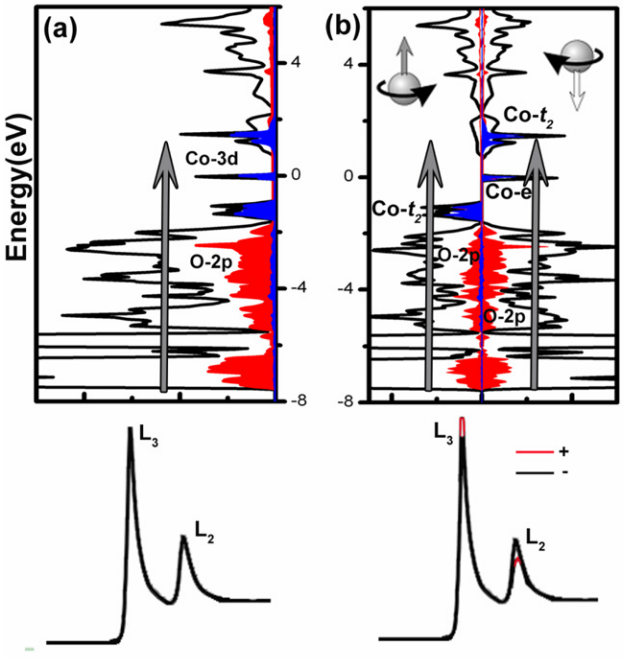

Figure 3. (a) Schematic of electron transitions accounting for the conventional Co-L edge (shown as below) recorded at non-chirality positions; (b) schematic to illustrate the origination of the difference spectra at two chiral positions (shown as below) in Co-doped ZnO. The straight arrows (gray) represent the excitation direction. The red and blue colors represent the initial 2*p* states and final Co-3*d* states, respectively. (For interpretation of the references to color in this figure legend, the reader is referred to the web version of this article.)

In conclusion, EMCD experiments were performed on synthesized cobalt-doped ZnO nanostructures and indicated that the ferromagnetism observed is intrinsic. The electronic structure of cobalt-doped ZnO was obtained from first-principles calculations, and the electronic states contributing to the spin imbalance were

identified. Based on the theoretical calculation, an exact model is proposed which correlates the dichroism observed in cobalt-doped ZnO with its electronic structure.

(1) Conventional electron energy loss spectroscopy, correlated with the non-spin-polarized density of states, was obtained from the electronic transitions from 2*p* states to empty Co-3*d* states above the Fermi level. The transition intensity from the O-2*p* states to the Co-3*d* states, measured as white line intensity, is proportional to the number of *d* holes.

(2) Electron magnetic chiral dichroism, correlated with the spin-polarized density of states, was obtained from the difference in the transition intensities from the spin-polarized 2*p* states to Co-3*d* states. Thus the spin imbalance (mainly from the Co-3*d* states) in the conduction band of cobalt-doped ZnO can be measured.

Thus, the EMCD measurements performed with TEM open the door for magnetic studies in ZnO-based dilute magnetic semiconductors.

This work was sponsored by the National Natural Science Foundation of China under Grant Nos. 50902014 and 51002017. Q.L. acknowledges the financial support from RGC of HKSAR under Grant No. 402007.

[1] S.A. Wolf, D.D. Awschalom, R.A. Buhrman, J.M. Daughton, S. Von Molnr, M.L. Roukes, A.Y. Chtchelkanova, D.M. Treger, Science 294 (2001) 1488.
[2] P. Sharma, A. Gupta, K.V. Rao, F.J. Owens, R. Sharma, R. Ahuja, J.M.O. Guillen, B. Johansson, G.A. Gehring, Nat. Mater. 2 (2003) 673.
[3] K.R. Kittilstved, W.K. Lin, D.R. Gamelin, Nat. Mater. 5 (2006) 291.
[4] P.V. Radovanovic, D.R. Gamelin, Phys. Rev. Lett. 91 (2003) 157202.
[5] J.W. Quilty, A. Shibata, J.Y. Son, K. Takubo, T. Mizokawa, H. Toyosaki, T. Fukumura, M. Kawasaki, Phys. Rev. Lett. 96 (2006) 027202.
[6] J.R. Neal, A.J. Behan, R.M. Ibrahim, H.J. Blythe, M. Ziese, A.M. Fox, G.A. Gehring, Phys. Rev. Lett. 96 (2006) 197208.
[7] P. Schattschneider, S. Rubino, C. Hébert, J. Rusz, J. Kuneš, P. Novák, E. Carlino, M. Fabrizioli, G. Panaccione, G. Rossi, Nature 441 (2006) 486.
[8] Z.H. Zhang, X.F. Wang, J.B. Xu, S. Muller, C. Ronning, Q. Li, Nat. Nanotechnol. 4 (2009) 523.
[9] X.F. Wang, J.B. Xu, B. Zhang, H.G. Yu, J. Wang, X.X. Zhang, J.G. Yu, Q. Li, Adv. Mater. 18 (2006) 2476.
[10] X.F. Wang, F.Q. Song, Q. Chen, T.Y. Wang, J.L. Wang, P. Liu, M.R. Shen, J.G. Wan, G.H. Wang, J.B. Xu, J. Am. Chem. Soc. 132 (2010) 6492.
[11] P. Blaha, K. Schwarz, G.K.H. Madsen, D. Kvasnicka, J. Luitz, WIEN2K, An Augmented Plane Wave + Local Orbitals Program for Calculating Crystal Properties, Techn. Universität, Wien, 2001.
[12] J.P. Perdew, K. Burke, M. Ernzerhof, Phys. Rev. Lett. 77 (1996) 3865.
[13] Z.H. Zhang, X.Y. Qi, J.K. Jian, X.F. Duan, Micron 37 (2006) 229.
[14] A. Walsh, Juarez L.F. Da Silva, S.H. Wei, Phys. Rev. Lett. 100 (2008) 256401.
[15] R.F. Egerton, Electron Energy Loss Spectroscopy in the Electron Microscope, Plenum Press, New York, 1996.